Unfolding Thermodynamics of Trp-Cage, a 20 Residue Miniprotein, Studied by Differential Scanning Calorimetry and Circular Dichroism Spectroscopy†

Werner W. Streicher‡ and George I. Makhatadze*,‡,§

Department of Biochemistry and Molecular Biology, The Pennsylvania State University College of Medicine, Hershey, Pennsylvania 17033, and Department of Chemistry, The Pennsylvania State University, University Park, Pennsylvania 16802

Received November 22, 2006; Revised Manuscript Received January 5, 2007

ABSTRACT: Small proteins provide convenient models for computational studies of protein folding and stability, which are usually compared with experimental data. Until recently, the unfolding of Trp-cage was considered to be a two-state process. However, no direct experimental evidence for this has been presented, and in some cases, the contrary has been suggested. To elucidate a detailed unfolding mechanism, we studied the thermodynamics of unfolding of Trp-cage by differential scanning calorimetry (DSC) and circular dichroism (CD) spectroscopy. The observation that at low temperatures only ∼90−95% of Trp-cage exists in the native conformation presented an analytical challenge. Nevertheless, it was found that the DSC and CD data can be fitted simultaneously to the same set of thermodynamic parameters. The major uncertainty in such a global fit is the heat capacity change upon unfolding, ΔC_p. This can be circumvented by obtaining ΔC_p directly from the difference between heat capacity functions of the native and unfolded states. Using such an analysis it is shown that Trp-cage unfolding can be represented by a two-state model with the following thermodynamic parameters: $T_m = 43.9 \pm 0.8$ °C, $\Delta H(T_m) = 56 \pm 2$ kJ/mol, $\Delta C_p = 0.3 \pm 0.1$ kJ/(mol·K). Using these thermodynamic parameters it is estimated that Trp-cage is marginally stable at 25 °C, $\Delta G(25\ °C) = 3.2 \pm 0.2$ kJ/mol, which is only 30% more than the thermal fluctuation energy at this temperature.

The discovery of rapidly folding small proteins and peptides has narrowed the gap between protein folding computational studies and experiment, as the faster experimentally determined time scales have become more feasible for computational studies (*1*). Model peptides for these studies are isolated regions of different proteins (*2*−*6*). A major limitation is the modest population of natively folded structures and/or aggregation, in the absence of cosolvents, that occur when the peptide is no longer within the tertiary structural context of the protein. To remedy this, peptides have been redesigned to improve their solubility and the extent of native structure formation without the requirement of cofactors or organic cosolvents. A prime example of this strategy is the design of Trp-cage.

Trp-cage is a synthetic 20-residue peptide based on the 39-residue peptide exendin-4 from the Gila monster saliva (*7*). By truncating the exendin-4 N-terminal region by 19 residues and substituting a further 5 residues, the authors were able to construct a monomeric peptide which is folded in solution. The structure of Trp-cage was solved by NMR, and it showed that the peptide consists of an α-helix (residues 2−8), a short 3_{10}-helix (residues 11−14), and a polyproline II helix at the C-terminus. The interactions between Tyr3, Trp6, Gly11, Pro12, Pro18, and Pro19 constitute the Trp-cage fold and impart tertiary structural characteristics on the peptide giving it features of a "miniprotein".

Thermal unfolding of Trp-cage was monitored using different spectroscopic methods which all indicate that Trp-cage unfolds in a cooperative two-state process (*7*, *8*). However, in 2005 Ahmed et al., using UV-resonance Raman spectroscopy, suggested that an intermediate is formed during the thermal unfolding of Trp-cage and that Trp-cage does not unfold in a two-state process. Folding kinetics experiments have shown that Trp-cage folds with two-state kinetics and is, to date, the fastest folding "protein" with a folding rate of 4 μs (*8*). On the other hand, by probing the folding dynamics of Trp-cage using a fluorescent tag, Neuweiler et al. (*9*) suggested that Trp-cage forms a molten globule-like intermediate, which enhances the folding rate. Even though the small size of Trp-cage and its exceptionally fast folding rate have made it a very attractive model for computational studies (*10*−*22*), the question of whether or not the unfolding of Trp-cage is a two-state process has not been specifically addressed experimentally. In order to investigate this question, we monitored the thermal unfolding of Trp-cage using a nonspectroscopic method, differential scanning calorimetry, as well as a spectroscopic method, far-UV circular dichroism.

MATERIALS AND METHODS

Peptide Synthesis and Purification. The Trp-cage peptide (NLYIQWLKDGGPSSGRPPPS) was synthesized using standard Fmoc chemistry at the Penn State Macromolecular Core Facility. The peptide was purified by reverse-phase HPLC using a C18 column and a 0−100% acetonitrile

† This work was supported by a grant (GM54537) from the National Institutes of Health.

* Corresponding author. Tel: (717) 531-0712. Fax: (717) 531-7072. E-mail: makhatadze@psu.edu.

‡ The Pennsylvania State University College of Medicine.

§ The Pennsylvania State University.

10.1021/bi602424x CCC: $37.00
Published on Web 02/13/2007

gradient in the presence of 0.065−0.05% TFA. After HPLC, fractions containing peptide were pooled, lyophilized, and resuspended in deionized water, and the process was repeated to remove residual TFA. Peptide purity and identity were confirmed by MADLI-TOF (data not shown). Trp-cage concentration was determined spectroscopically at 280 nm using an extinction coefficient of $\epsilon_{280,0.1\%} = 3.24$ o.u., where o.u. stands for optical units. The peptide was equilibrated into either 20 mM sodium phosphate or 20 mM sodium cacodylate, both at pH 7.0, using a Sephadex G-10 column (1 cm diameter × 50 cm), prior to DSC[1] or CD.

Analytical Equilibrium Ultracentrifugation. Analytical ultracentrifugation experiments were performed using a Beckman XLA centrifuge. Profiles were collected at 280 nm. All experiments were performed at 4 °C and at 35000 rpm in 20 mM sodium phosphate or 20 mM sodium cacodylate, both at pH 7.0. The data were fitted using nonlinear regression software (NLREG) to the following equation, which describes the distribution of a single ideal species at equilibrium:

$$C_r = C_{r_0}\left[\frac{\omega^2}{2RT}M(1 - \bar{\nu}\rho)(r^2 - r_0^2)\right] \quad (1)$$

where C_r is the peptide concentration at radius r, C_{r_0} is the concentration of monomeric peptide at r_0, ω is the angular velocity, R is the gas constant [8.134 × 107 erg/(mol·K)], T is the temperature in kelvin, M is the monomer molecular weight, $\bar{\nu}$ is the partial specific volume of the solute, and ρ is the density of the solvent (equal to 1 g/cm^3). From the fitted data, the molecular weight of Trp-cage was found to be 2.1 ± 0.1 kDa, which is consistent with the predicted molecular weight based on the amino acid composition for monomeric Trp-cage.

Circular Dichroism (CD) Spectroscopy. CD measurements were performed on a Jasco J-715 spectrapolarimeter. All measurements were carried out using a 1 mm water-jacketed cylindrical quartz cell, and the temperature was regulated by an automated circulating water bath. Far-UV CD spectra were measured from 250 to 190 from 2 to 97 °C at 5 °C increments. Ellipticity values (Θ) were converted to mean residue ellipticity ([Θ] in deg cm^2 dmol^{-1}) using

$$[\Theta] = \Theta\mathrm{MR}/(10lc) \quad (2)$$

where MR is the mean molecular mass of the amino acids (for Trp-cage MR = 108.47), l is the light path length in centimeters, and c is the peptide concentration in milligrams per milliliter. The far-UV CD spectra show a minimum ellipticity at 222 nm indicative of α-helical structure, and this wavelength was used to monitor the temperature-induced unfolding of Trp-cage. For CD unfolding, peptide concentrations were ∼0.1 mg/mL in 20 mM sodium phosphate or 20 mM sodium cacodylate, pH 7.0. Reversibility studies were performed by measuring the far-UV CD spectrum of the peptide at 2 °C after unfolding at high temperatures (reversibility was found to be >90%).

Differential Scanning Calorimetry (DSC). DSC experiments were performed using a VP-DSC instrument (Microcal Inc.) at Trp-cage concentrations from 1 to 1.3 mg/mL with a scan rate of 90 deg/h (as described in refs *23* and *24*). Unfolding was performed in 20 mM sodium phosphate or 20 mM sodium cacodylate, both at pH 7.0. The partial molar heat capacity of Trp-cage in solution was calculated to be 0.706 cm^3/g (*25*). Reversibility was determined by repeating the experiment on the same sample and was found to be >98%.

Data Analysis. The DSC and CD data were fitted simultaneously (global fit) to a monomolecular two-state unfolding model where only native (N) and unfolded (U) states significantly populate the thermal unfolding transition. For a two-state unfolding model, the enthalpy of unfolding (ΔH), the heat capacity change upon unfolding (ΔC_p), and the transition temperature (T_m) are sufficient thermodynamic parameters to describe the unfolding process (*26*, *27*).

The relationship between Gibbs free energy (ΔG), ΔH, and ΔS is described by

$$\Delta G(T) = \Delta H(T) - T\Delta S(T) \quad (3)$$

where ΔH and ΔS are the enthalpy and entropy changes of peptide unfolding, respectively. The temperature dependence of ΔH and ΔS is defined by the heat capacity change upon unfolding, ΔC_p, as follows:

$$\Delta C_p = \frac{\mathrm{d}\Delta H(T)}{\mathrm{d}T} = T\frac{\mathrm{d}\Delta S(T)}{\mathrm{d}T} \quad (4)$$

If ΔC_p is independent of temperature, the temperature dependence of the Gibbs free energy can be defined as

$$\Delta G(T) = \frac{T_m - T}{T_m}\Delta H(T_m) + \Delta C_p(T - T_m) + T\Delta C_p \ln\left(\frac{T_m}{T}\right) \quad (5)$$

The CD and DSC data were fitted simultaneously to eq 5 using nonlinear regression software (NLREG). In general, two independent enthalpies, namely, the fitted enthalpy, $\Delta H(T_m)$, and the calorimetric enthalpy, $\Delta H_{cal}(T_m)$, can be determined directly from a single DSC experiment (*26*, *27*). If the $\Delta H(T_m)$ and $\Delta H_{cal}(T_m)$ are the same, the thermal unfolding is closely approximated by a two-state process. For this reason, DSC is the method of choice when determining the mode of unfolding. However, in the case of Trp-cage, the $\Delta H_{cal}(T_m)$ could not be evaluated as the native state baseline could not be determined directly from the experimental data because the native state population never reaches 100% in the studied temperature range (see below).

RESULTS AND DISCUSSION

Figure 1A,B shows the temperature-induced unfolding profiles for Trp-cage as monitored by circular dichroism (CD) spectroscopy and differential scanning calorimetry (DSC). Inspection of the profiles suggests that even at low temperatures Trp-cage does not appear to be 100% native. This is consistent with the original observations by Neidigh et al. (*7*), that provided NMR evidence that Trp-cage is 95% native at 4 °C. Analyzing the unfolding profiles without a well-defined native state baseline presents a formidable challenge, particularly when the mode of unfolding is not well defined.

[1] Abbreviations: DSC, differential scanning calorimetry; CD, circular dichroism; NMR, nuclear magnetic resonance.

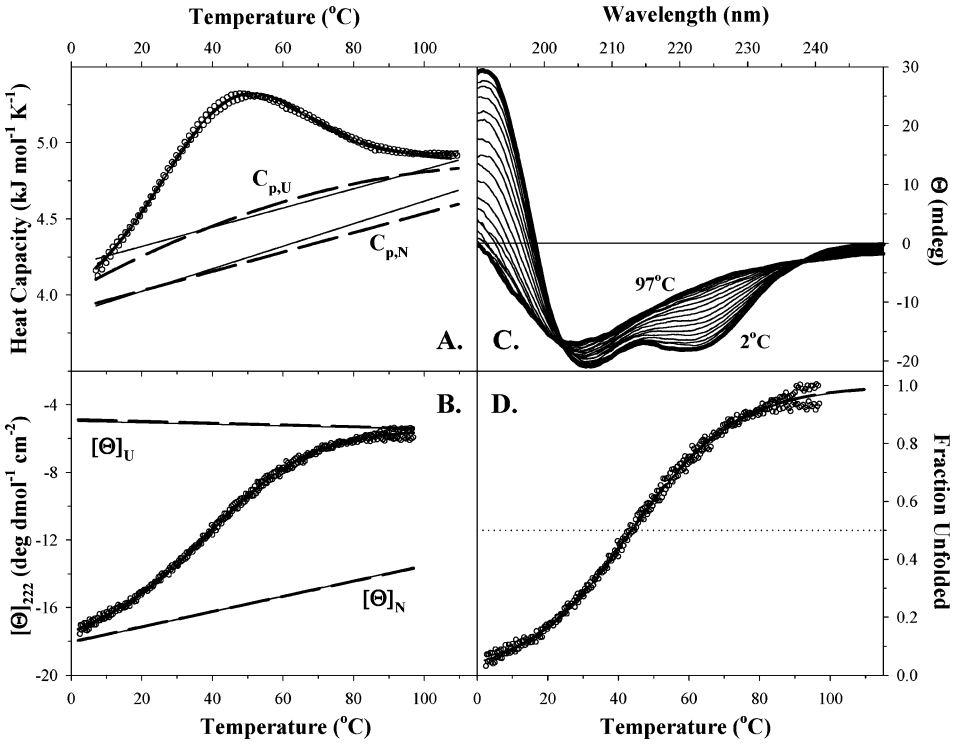

FIGURE 1: Temperature-induced unfolding of Trp-cage. Panel A: Thermal unfolding of Trp-cage monitored using DSC in 20 mM sodium phosphate or 20 mM sodium cacodylate, pH 7.0 (○). The solid lines represent the fit to a two-state model. The dashed lines show the positions of the unfolded state baseline ($C_{p,U}$) and the native state baseline ($C_{p,N}$) where $C_{p,U}$ was nonlinear. Panel B: Thermal unfolding of Trp-cage monitored using far-UV CD at 222 nm in 20 mM sodium phosphate or 20 mM sodium cacodylate, pH 7.0 (○). The solid line represents the fit to a two-state model, and $[\Theta]_U$ and $[\Theta]_N$ represent the unfolded and native state baselines, respectively. Panel C: Far-UV CD spectra from 2 to 97 °C at 5 °C increments showing the isodichroic point at ~203 nm. Panel D: Fraction unfolded for CD data (thin solid line) and DSC data (dashed line), both fitted to a two-state unfolding model. The open symbols (○) represent the experimental CD fraction unfolded in 20 mM sodium phosphate or 20 mM sodium cacodylate, pH 7.0.

The temperature dependence of the CD spectra (Figure 1C) shows a well-developed isodichroic point that is often considered to be indicative of a two-state process (*28*). Consequently, we asked the question whether a single set of thermodynamic parameters could simultaneously describe the DSC and CD unfolding profiles according to a two-state model, where the monomeric native state (N) unfolds to yield the unfolded state (U; as described by N ↔ U), and if so, does the global fit produce reasonable values for the native and unfolded state baselines. When the global fitting routine had 11 parameters [8 parameters describing the linear dependences for the native and unfolded states for CD and DSC, in addition to the transition temperature, T_m, enthalpy of unfolding at T_m, $\Delta H(T_m)$, and heat capacity changes upon unfolding, ΔC_p], the values for the unfolded baselines, T_m and $\Delta H(T_m)$, remained almost unchanged, while there was an interdependence of the slope of the native state baselines and ΔC_p (data not shown). The interdependence of the native state baseline and ΔC_p suggests that one needs to determine one of the two parameters independently. Since ΔC_p is the difference between the heat capacity of a protein in the unfolded ($C_{p,U}$) and native states ($C_{p,N}$), the fitting routine was modified not to fit for ΔC_p implicitly, but as the difference between $C_{p,U}$ and $C_{p,N}$ (*29*). This explicit determination of ΔC_p leads to an excellent fit of both CD and DSC profiles (see Figure 1A,B), with the following parameters of unfolding, $T_m = 43.7 \pm 1.8$ °C, $\Delta H(T_m) = 56 \pm 2$ kJ/mol, and $\Delta C_p = 0.3 \pm 0.1$ kJ/mol, determined from the difference of $C_{p,U}$ and $C_{p,N}$.

Representation of the heat capacities of the native state as a linear function of temperature has been well justified experimentally (*30*−*34*). However, the linear temperature dependence of the heat capacity of the unfolded state is only applicable for proteins with large enthalpies of unfolding because the larger the enthalpy of a two-state transition, the narrower the temperature range of the unfolding transition (*30*). For Trp-cage the thermal unfolding transition seems to be rather broad, and thus the unfolded state baseline should be represented by a nonlinear function. It has been shown that the heat capacity of the unfolded polypeptide can be calculated from the amino acid composition as (*32*, *35*)

$$C_{p,U}^{calc}(T) = C_{p,-CHCONH-}(T)(n-1) + \sum_n C_{p,R_i}(T)n_i \quad (6)$$

where n is the total number of amino acid residues, n_i is the number of a given type of amino acid residue, $C_{p,-CHCONH-}(T)$ is the temperature dependence of the partial heat capacity of the peptide backbone, and $C_{p,R_i}(T)$ is the temperature dependence of the partial heat capacity of the individual amino acid side chain. The values of $C_{p,-CHCONH-}(T)$ and $C_{p,R_i}(T)$ have been determined previously for the temperature range from 5 to 125 °C (*32*, *35*). The $C_{p,U}^{calc}(T)$ for Trp-cage, calculated using eq 6, shows that at high temperatures $C_{p,U}^{calc}(T)$ is very close, within 0.2 kJ/(mol·K) or only 4% of the absolute value, to the heat capacity of the Trp-cage measured experimentally. As a result, this function was used in the global fit as the heat capacity of the unfolded state but was allowed to undergo vertical displacement. The results

of the global fit using the nonlinear dependence of the unfolded state baseline for the DSC profile is shown in Figure 1A. The thermodynamic parameters were found to be T_m = 43.9 ± 0.8 °C, $\Delta H(T_m)$ = 56 ± 1 kJ/mol, and ΔC_p = 0.25 ± 0.05 kJ/(mol·K), which is very similar to the values obtained when using a linear heat capacity for the unfolded state. Moreover, the two-state global fits, with different unfolded heat capacity functions, produce very similar heat capacity functions for the native state (Figure 1A). The T_m values obtained previously (approximately 42 °C; refs *7* and *8*) compare well with the T_m obtained using DSC and far-UV CD at 222 nm, taking into consideration the relatively broad thermal transition. This observation further argues that the unfolding is a two-state process, as two-state thermal transitions should yield similar thermodynamic parameters irrespective of the probe used to monitor the thermal unfolding process (*36*).

Figure 1D shows the population of the native and unfolded molecules calculated according to the global fit to a two-state model. Importantly, the model predicts that the native state is 92% populated at 4 °C, which is in excellent agreement with 95% previously estimated on the basis of NMR (*7*). Overall, the temperature-induced transition of Trp-cage is rather broad where the population of unfolded molecules will reach 99% above 100 °C (Figure 1D).

It is clear that the same set of thermodynamic parameters can simultaneously describe the CD and DSC thermal unfolding profiles according to a two-state model. The question is how realistic are the estimates for the native and unfolded state baselines. The native state and unfolded state baselines for the CD unfolding profile are within the range one would expect for a helix-containing peptide. For example, the slope for the native state is ~50 deg dmol^{-1} cm^{-2} per °C, which compares well with the slope of the temperature dependence of ellipticity for an α-helix (see, e.g., refs *37* and *38*), recognizing, however, that aromatic residues in Trp-cage might contribute (*39*, *40*). The negative slope for the unfolded state baseline is consistent with the temperature dependence of the CD signal for unfolded peptides (*37*). Similarly, the heat capacity for the unfolded state is consistent with the previous estimates (*24*, *32*, *38*, *41*, *42*). For example, the unfolded state heat capacity at high temperatures from the fitted data is estimated to be ~4.8 kJ/(mol·K) while calculations according to eq 6 give an estimate of 4.7 kJ/(mol·K). Similarly, the estimates for the value of $C_{p,U}$ from the fit, at 25 °C, are 4.31 and 4.35 kJ/(mol·K), based on the nonlinear and linear $C_{p,U}$ models, respectively, which compare well with the value of 4.2 kJ/(mol·K) calculated from eq 6. Moreover, the values for the unfolded state heat capacities are within the range obtained for other proteins. At 25 °C the specific heat capacity, expressed per gram of protein to facilitate the comparison, of Trp-cage is 1.98 J/(g·K) which is well within the range of 1.85−2.20 J/(g·K) reported for other proteins (*24*, *34*, *43*). The heat capacity of the native state of Trp-cage changes linearly with temperature with a slope of 7.5 J/(mol·K^2) or 0.4 J/(g·K^2). The specific value, calculated per gram of protein to facilitate comparison, of the temperature dependence of the heat capacity of the native state can be compared to the temperature dependences of small globular proteins such as BPTI, 0.56 J/(g·K^2), or barnase, 0.61 J/(g·K^2) (*33*, *44*). The absolute value of the heat capacity of the native state of Trp-cage at 25 °C is estimated to be 4.06 kJ/(mol·K) or 1.89 J/(g·K), which is somewhat larger than the known specific heat capacities of globular proteins ranging from 1.25 to 1.80 J/(g·K) (*24*, *34*, *43*). Consequently, the heat capacity change upon unfolding is rather small, only ~0.3 kJ/(mol·K). Such a small ΔC_p is probably due in part to the structural peculiarity of Trp-cage that has part of the molecule in the PPII conformation. For comparison, the heat capacity change upon unfolding is considered to be close to zero in collagen, where individual polypeptides that form a triple helix are in PPII conformation (see, e.g., ref *45*). The similarity with collagen can be further extended to the enthalpy of unfolding. For example, a $(PPG)_{10}$ sequence repeat forming a collagen triple helix unfolds at 32 °C with the enthalpy of unfolding of 179 kJ/mol, which translates to 2 kJ/mol per amino acid residue (*46*). This compares well with the 56 kJ/mol for the enthalpy of unfolding at 43 °C for Trp-cage, keeping in mind that Trp-cage has 5 or 6 out of 20 of its residues in the PPII conformation, and 6−7 residues forming an α-helix, another structural element that also has rather low enthalpy of unfolding (*37*, *38*, *47*−*49*).

Overall, it appears that the temperature-induced melting profiles of the Trp-cage miniprotein monitored by two independent methods (CD spectroscopy and DSC) can be fitted to a two-state model. The global fit not only allows the estimation of the thermodynamic parameters of unfolding but also allows one to obtain rather reliable estimates for the native state baselines that are otherwise undefined. This is only possible because of the independent semiempirical estimate of the heat capacity change on unfolding from the DSC profile. The obtained thermodynamic parameters estimate the stability of the Trp-cage miniprotein at 25 °C to be ΔG(25 °C) = 3.2 ± 0.2 kJ/mol, which is only 30% more than the thermal fluctuation energy at this temperature.

ACKNOWLEDGMENT

We thank Ann Stanley from the Penn State Macromolecular Core Facility for the synthesis of the Trp-cage peptide.

REFERENCES

1. Gnanakaran, S., Nymeyer, H., Portman, J., Sanbonmatsu, K. Y., and Garcia, A. E. (2003) Peptide folding simulations, *Curr. Opin. Struct. Biol. 13*, 168−174.
2. Cox, J. P., Evans, P. A., Packman, L. C., Williams, D. H., and Woolfson, D. N. (1993) Dissecting the structure of a partially folded protein. Circular dichroism and nuclear magnetic resonance studies of peptides from ubiquitin, *J. Mol. Biol. 234*, 483−492.
3. Nelson, J. W., and Kallenbach, N. R. (1986) Stabilization of the ribonuclease S-peptide alpha-helix by trifluoroethanol, *Proteins 1*, 211−217.
4. McKnight, C. J., Doering, D. S., Matsudaira, P. T., and Kim, P. S. (1996) A thermostable 35-residue subdomain within villin headpiece, *J. Mol. Biol. 260*, 126−134.
5. Tang, Y., Rigotti, D. J., Fairman, R., and Raleigh, D. P. (2004) Peptide models provide evidence for significant structure in the denatured state of a rapidly folding protein: the villin headpiece subdomain, *Biochemistry 43*, 3264−3272.
6. Bunagan, M. R., Yang, X., Saven, J. G., and Gai, F. (2006) Ultrafast folding of a computationally designed Trp-cage mutant: Trp2-cage, *J. Phys. Chem. B 110*, 3759−3763.
7. Neidigh, J. W., Fesinmeyer, R. M., and Andersen, N. H. (2002) Designing a 20-residue protein, *Nat. Struct. Biol. 9*, 425−430.
8. Qiu, L., Pabit, S. A., Roitberg, A. E., and Hagen, S. J. (2002) Smaller and faster: the 20-residue Trp-cage protein folds in 4 μs, *J. Am. Chem. Soc. 124*, 12952−12953.
9. Neuweiler, H., Doose, S., and Sauer, M. (2005) A microscopic view of miniprotein folding: enhanced folding efficiency through

formation of an intermediate, *Proc. Natl. Acad. Sci. U.S.A. 102*, 16650−16655.
10. Snow, C. D., Zagrovic, B., and Pande, V. S. (2002) The Trp cage: folding kinetics and unfolded state topology via molecular dynamics simulations, *J. Am. Chem. Soc. 124*, 14548−14549.
11. Chowdhury, S., Lee, M. C., Xiong, G., and Duan, Y. (2003) Ab initio folding simulation of the Trp-cage mini-protein approaches NMR resolution, *J. Mol. Biol. 327*, 711−717.
12. Pitera, J. W., and Swope, W. (2003) Understanding folding and design: replica-exchange simulations of "Trp-cage" miniproteins, *Proc. Natl. Acad. Sci. U.S.A. 100*, 7587−7592.
13. Nikiforovich, G. V., Andersen, N. H., Fesinmeyer, R. M., and Frieden, C. (2003) Possible locally driven folding pathways of TC5b, a 20-residue protein, *Proteins 52*, 292−302.
14. Zagrovic, B., and Pande, V. (2003) Solvent viscosity dependence of the folding rate of a small protein: distributed computing study, *J. Comput. Chem. 24*, 1432−1436.
15. Zhou, R. (2003) Trp-cage: folding free energy landscape in explicit water, *Proc. Natl. Acad. Sci. U.S.A. 100*, 13280−13285.
16. Zhou, R. (2004) Exploring the protein folding free energy landscape: coupling replica exchange method with P3ME/RESPA algorithm, *J. Mol. Graphics Modell. 22*, 451−463.
17. Ding, F., Buldyrev, S. V., and Dokholyan, N. V. (2005) Folding Trp-cage to NMR resolution native structure using a coarse-grained protein model, *Biophys. J. 88*, 147−155.
18. Irback, A., and Mohanty, S. (2005) Folding thermodynamics of peptides, *Biophys. J. 88*, 1560−1569.
19. Schug, A., and Wenzel, W. (2006) An evolutionary strategy for all-atom folding of the 60-amino-acid bacterial ribosomal protein l20, *Biophys. J. 90*, 4273−4280.
20. Schug, A., Wenzel, W., and Hansmann, U. H. (2005) Energy landscape paving simulations of the Trp-cage protein, *J. Chem. Phys. 122*, 194711−194717.
21. Chen, J., Im, W., and Brooks, C. L., III (2006) Balancing solvation and intramolecular interactions: toward a consistent generalized Born force field, *J. Am. Chem. Soc. 128*, 3728−3736.
22. Juraszek, J., and Bolhuis, P. G. (2006) Sampling the multiple folding mechanisms of Trp-cage in explicit solvent, *Proc. Natl. Acad. Sci.U.S.A. 103*, 15859−15864.
23. Makhatadze, G. I. (1998) *Measuring protein thermostability by differential scanning calorimetry*, Vol. 2, John Wiley & Sons, New York.
24. Streicher, W. W., and Makhatadze, G. I. (2007) Advances in the analysis of conformational transitions in peptides using differential scanning calorimetry, *Methods Mol. Biol. 350*, 105−113.
25. Makhatadze, G. I., Medvedkin, V. N., and Privalov, P. L. (1990) Partial molar volumes of polypeptides and their constituent groups in aqueous solution over a broad temperature range, *Biopolymers 30*, 1001−1010.
26. Privalov, P. L., and Potekhin, S. A. (1986) Scanning microcalorimetry in studying temperature-induced changes in proteins, *Methods Enzymol. 131*, 4−51.
27. Biltonen, R. L., and Freire, E. (1978) Thermodynamic characterization of conformational states of biological macromolecules using differential scanning calorimetry, *CRC Crit. Rev. Biochem. 5*, 85−124.
28. Holtzer, M. E., and Holtzer, A. (1992) Alpha-helix to random coil transitions: determination of peptide concentration from the CD at the isodichroic point, *Biopolymers 32*, 1675−1677.
29. Pace, C. N., Grimsley, G. R., Thomas, S. T., and Makhatadze, G. I. (1999) Heat capacity change for ribonuclease A folding, *Protein Sci. 8*, 1500−1504.
30. Privalov, P. L. (1979) Stability of proteins: small globular proteins, *Adv. Protein Chem. 33*, 167−241.
31. Privalov, P. L., Tiktopulo, E. I., Venyaminov, S., Griko Yu, V., Makhatadze, G. I., and Khechinashvili, N. N. (1989) Heat capacity and conformation of proteins in the denatured state, *J. Mol. Biol. 205*, 737−750.
32. Privalov, P. L., and Makhatadze, G. I. (1990) Heat capacity of proteins. II. Partial molar heat capacity of the unfolded polypeptide chain of proteins: protein unfolding effects, *J. Mol. Biol. 213*, 385−391.
33. Makhatadze, G. I., Kim, K. S., Woodward, C., and Privalov, P. L. (1993) Thermodynamics of BPTI folding, *Protein Sci. 2*, 2028−2036.
34. Lopez, M. M., and Makhatadze, G. I. (2002) Differential scanning calorimetry, *Methods Mol. Biol. 173*, 113−119.
35. Makhatadze, G. I., and Privalov, P. L. (1990) Heat capacity of proteins. I. Partial molar heat capacity of individual amino acid residues in aqueous solution: hydration effect, *J. Mol. Biol. 213*, 375−384.
36. Ginsburg, A., and Carroll, W. R. (1965) Some specific ion effects on the conformation and thermal stability of ribonuclease, *Biochemistry 4*, 2159−2174.
37. Rohl, C. A., and Baldwin, R. L. (1998) Deciphering rules of helix stability in peptides, *Methods Enzymol. 295*, 1−26.
38. Richardson, J. M., and Makhatadze, G. I. (2004) Temperature dependence of the thermodynamics of helix-coil transition, *J. Mol. Biol. 335*, 1029−1037.
39. Chakrabartty, A., Kortemme, T., Padmanabhan, S., and Baldwin, R. L. (1993) Aromatic side-chain contribution to far-ultraviolet circular dichroism of helical peptides and its effect on measurement of helix propensities, *Biochemistry 32*, 5560−5565.
40. Vuilleumier, S., Sancho, J., Loewenthal, R., and Fersht, A. R. (1993) Circular dichroism studies of barnase and its mutants: characterization of the contribution of aromatic side chains, *Biochemistry 32*, 10303−10313.
41. Makhatadze, G. I. (1998) Heat capacities of amino acids, peptides and proteins, *Biophys. Chem. 71*, 133−156.
42. Streicher, W. W., and Makhatadze, G. I. (2006) Calorimetric evidence for a two-state unfolding of the beta-hairpin peptide trpzip4, *J. Am. Chem. Soc. 128*, 30−31.
43. Privalov, P. L., and Dragan, A. I. (2006) Microcalorimetry of biological macromolecules, *Biophys. Chem.* (in press).
44. Griko, Y. V., Makhatadze, G. I., Privalov, P. L., and Hartley, R. W. (1994) Thermodynamics of barnase unfolding, *Protein Sci. 3*, 669−676.
45. Privalov, P. L. (1982) Stability of proteins. Proteins which do not present a single cooperative system, *Adv. Protein Chem. 35*, 1−104.
46. Persikov, A. V., Xu, Y., and Brodsky, B. (2004) Equilibrium thermal transitions of collagen model peptides, *Protein Sci. 13*, 893−902.
47. Richardson, J. M., McMahon, K. W., MacDonald, C. C., and Makhatadze, G. I. (1999) MEARA sequence repeat of human CstF-64 polyadenylation factor is helical in solution. A spectroscopic and calorimetric study, *Biochemistry 38*, 12869−12875.
48. Richardson, J. M., Lopez, M. M., and Makhatadze, G. I. (2005) Enthalpy of helix-coil transition: missing link in rationalizing the thermodynamics of helix-forming propensities of the amino acid residues, *Proc. Natl. Acad. Sci. U.S.A. 102*, 1413−1418.
49. Lopez, M. M., Chin, D. H., Baldwin, R. L., and Makhatadze, G. I. (2002) The enthalpy of the alanine peptide helix measured by isothermal titration calorimetry using metal-binding to induce helix formation, *Proc. Natl. Acad. Sci. U.S.A. 99*, 1298−1302.

BI602424X